Original Article

Mol Imaging Radionucl Ther 2026;35(1):35-43 **DOI:***10.4274/mirt.galenos.2025.92259*

Quantitative characterization of ^{18}F-PSMA-1007 and [^{68}Ga]Ga-PSMA-11 PET-CT Imaging in Suspected Prostate Cancer: A Single-centre Experience

Şüpheli Prostat Kanserinde ^{18}F-PSMA-1007 ve [^{68}Ga]Ga-PSMA-11 PET-BT Görüntülemesinin Kantitatif Karakterizasyonu: Tek Merkezli Bir Deneyim

Bal Sanghera[1], Gerry Lowe[2], Sophie Sanghera[3], Wai Lup Wong[4]

[1]*St. Barts Health Nhs Trust, Clinic of Nuclear Medicine, London, United Kingdom*
[2]*Paul Strickland Scanner Centre, Clinic of Pet Physics, Northwood, United Kingdom*
[3]*King College London Faculty of Medicine, Department of Physics, London, United Kingdom*
[4]*Paul Strickland Scanner Centre, Clinic of Radiology, Northwood, United Kingdom*

Abstract

Objectives: We record quantitative differences between ^{18}F-prostate specific membrane antigen (^{18}F-PSMA)-1007 and [^{68}Ga]Ga-PSMA-11 positron emission tomography (PET) prostate scans at our centre to investigate if significant differences exist between suspected lesion and lesion/background parameters studied. We also assess the potential impact of such differences on tracer interchangeability when supply is constrained.

Methods: Sixty-one [^{68}Ga]Ga-PSMA-11 and seventy-two ^{18}F-PSMA-1007 patients were analysed in two cohorts, each comprising 200 lesions. Clinical reports were used to determine maximum standard uptake values (SUV_{max}) was recorded for suspected lesions (T). Similarly, normalisations of mean standardized uptake (SUV_{mean}) and standardized uptake value-peak (SUV_{peak}) using lean body mass (SUV_{lbm}) and body surface area (SUV_{bsa}) were estimated. SUV_{mean} of liver backgrounds (B) was recorded to estimate T/B ratios. Metabolic tumour volume and total lesion PSMA (TL-PSMA) were investigated as functional volume surrogates. The Mann-Whitney U test was used to identify significant differences between the [^{68}Ga]Ga-PSMA-11 and ^{18}F-PSMA-1007 distributions.

Results: Significant differences were observed for lesion SUV_{max} ($p=0.0004$), SUV_{peak} ($p=0.0017$), SUV_{mean} ($p=0.0007$), SUV_{lbm} ($p=0.0002$), and SUV_{bsa} ($p=0.0005$) in lesions with higher [^{68}Ga]Ga-PSMA-11 SUV. Similarly, significant differences were observed in liver SUV_{max} ($p<0.0001$), SUV_{peak} ($p<0.0001$), and SUV_{mean} ($p<0.0001$), with higher values for ^{18}F-PSMA-1007. T/B ($p<0.0001$) and TL-PSMA ($p=0.0063$) also exhibited significantly higher [^{68}Ga]Ga-PSMA-11 values.

Conclusion: Consistent, predictable, and significant differences were observed in ^{18}F-PSMA-1007 and [^{68}Ga]Ga-PSMA-11 PET scans of lesion, liver, volume surrogates, supporting tracer interchangeability for patients with suspected prostate cancer. Our results also support the recent commissioning of PSMA-based PET tracers in England.

Keywords: PET-CT, prostate, fluorine radioisotopes, gallium radioisotopes, quantitative evaluation, PSMA-1007, Gallium-68 PSMA-11

Address for Correspondence: Bal Sanghera, St. Barts Health Nhs Trust, Clinic of Nuclear Medicine, London, United Kingdom
E-mail: bal.sanghera@nhs.net **ORCID ID:** orcid.org/0000-0003-0206-7834
Received: 16.06.2025 **Accepted:** 21.12.2025 **Publication Date:** 03.02.2026

Cite this article as: Sanghera B, Lowe G, Sanghera S, Wong WL. Quantitative characterization of ^{18}F-PSMA-1007 and [^{68}Ga]Ga-PSMA-11 PET-CT imaging in suspected prostate cancer: a single-centre experience. Mol Imaging Radionucl Ther. 2026;35(1):35-43.

Öz

Amaç: Merkezimizde, ^{18}F-prostat spesifik membran antijeni (^{18}F-PSMA)-1007 ile [^{68}Ga]Ga-PSMA-11 pozitron emisyon tomografisi (PET) prostat görüntülemeleri arasındaki nicel farklılıkları kaydederek, şüpheli lezyonlar ile lezyon/arka plan parametreleri arasında anlamlı farklar olup olmadığını araştırmayı amaçladık. Ayrıca, tedarik kısıtlı olduğunda bu farklılıkların radyofarmasötiklerin birbirinin yerine kullanılabilirliği üzerindeki olası etkisini değerlendirdik.

Yöntem: İki kohortta incelenmek üzere, 61 adet [^{68}Ga]Ga-PSMA-11 ve 72 adet ^{18}F-PSMA-1007 hastası analiz edildi; her kohort 200 lezyon içermekteydi. Klinik raporlar kullanılarak şüpheli lezyonlar (T) için maksimum standart tutulum değeri (SUV_{maks}) kaydedildi. Benzer şekilde, ortalama standart tutulum ($SUV_{ortalama}$) ve standart tutulum değeri-tepe (SUV_{zirve}), yağsız vücut kütlesi (SUV_{lbm}) ve vücut yüzey alanı (SUV_{bsa}) ile normalize edilerek hesaplandı. T/B (tümör/arka plan) oranlarını tahmin etmek amacıyla karaciğer arka planlarının $SUV_{ortalama}$ değerleri kaydedildi. Metabolik tümör hacmi ve toplam lezyon PSMA (TL-PSMA), fonksiyonel hacim göstergeleri olarak incelendi. [^{68}Ga]Ga-PSMA-11 ile ^{18}F-PSMA-1007 dağılımları arasındaki anlamlı farkları belirlemek için Mann-Whitney U testi kullanıldı.

Bulgular: Lezyon SUV_{maks} (p=0,0004), SUV_{zirve} (p=0,0017), $SUV_{ortalama}$ (p=0,0007), SUV_{lbm} (p=0,0002) ve SUV_{bsa} (p=0,0005) değerlerinde, daha yüksek [^{68}Ga]Ga-PSMA-11 SUV'u olan lezyonlarda anlamlı farklar gözlendi. Benzer şekilde, karaciğer SUV_{maks} (p<0,0001), SUV_{zirve} (p<0,0001) ve $SUV_{ortalama}$ (p<0,0001) değerlerinde de anlamlı farklar saptandı ve bu değerler ^{18}F-PSMA-1007 için daha yüksekti. T/B oranı (p<0,0001) ve TL-PSMA (p=0,0063) da anlamlı olarak daha yüksek [^{68}Ga]Ga-PSMA-11 değerleri gösterdi.

Sonuç: ^{18}F-PSMA-1007 ve [^{68}Ga]Ga-PSMA-11 PET görüntülemelerinde lezyon, karaciğer ve hacim göstergelerine ilişkin tutarlı, öngörülebilir ve anlamlı farklılıklar gözlenmiştir. Bu bulgular, prostat kanseri şüphesi olan hastalarda radyofarmasötiklerin birbirinin yerine kullanılabilirliğini desteklemektedir. Sonuçlarımız ayrıca İngiltere'de PSMA tabanlı PET radyofarmasötiklerinin yakın zamanda devreye alınmasını da desteklemektedir.

Anahtar kelimeler: PET-BT, prostat, flor radyoizotopları, galyum radyoizotopları, nicel değerlendirme, PSMA-1007, Galyum-68 PSMA-11

Introduction

Prostate cancer is the most frequently diagnosed cancer and the second most common cause of death among males in the United Kingdom (UK) (1). The most widely used positron emission tomography/computed tomography (PET/CT) oncology imaging agent in England is ^{18}F-fluorodeoxyglucose but it has limitations in diagnosing prostate cancer (2). In contrast, prostate specific membrane antigen (PSMA) imaging agents, such as [^{68}Ga]Ga-PSMA and ^{18}F-PSMA, have shown promise in clinical practice (3,4) and in targeted radioligand therapy applications (5). New prostate cancer-targeted PET imaging agents continue to be developed (6,7,8,9) while ^{99m}Tc-labelled PSMA ligands for single-photon emission tomography have also been explored for logistical reasons (10).

Availability of PET imaging agents is often limited in the UK, leading to diagnostic delays. Generator-eluted [^{68}Ga]Ga-PSMA-11, with a short half-life (~68 minutes), has been used widely because of its availability. However, ^{18}F-PSMA-1007, with a longer half-life (~110 minutes), offers greater geographic availability. This may address regional supply inequities while receiving substantial clinical support.

Many prostate cancer imaging studies have focused on the efficacy of radiopharmaceuticals using qualitative parameters such as detectability. However, more recent investigations have compared quantitative differences and their potential impact on analyses (11,12). For example, the VISION prostate cancer trial (13,14) incorporates lutetium-177 (^{177}Lu) Lu-PSMA-617 therapy and defines positive lesions as those with lesion-to-liver uptake ratios tumor-to-background (T/B) >1 measured on ^{68}Ga-PSMA-11 PET/CT scans.

However, different biodistribution effects have been identified between ^{18}F-PSMA-1007 and [^{68}Ga]Ga-PSMA-11 uptake in prostate cancer, leading to significant differences in lesion maximum standard uptake values (SUV_{max}). Increased hepatic excretion results in significantly higher ^{18}F-PSMA-1007 liver mean standardized uptake (SUV_{mean}), and similar significant differences are observed in the blood pool and spleen (4). Caution is therefore advised when the liver is used as a background tissue in T/B ratio estimation and when tracers are interchanged due to supply shortages. Characterising PET/CT quantitative parameters is essential for interpreting the clinical consequences of using different tracers. This highlights the importance of precise quantitative PET investigations (15,16).

In this study, routine clinically referred PET/CT scans using ^{18}F-PSMA-1007 and [^{68}Ga]Ga-PSMA-11 for suspected prostate cancer are characterised. Quantitative differences between radiopharmaceuticals are recorded, and their clinical implications are discussed, particularly when radiopharmaceuticals are interchanged. Ideally, the results of this local quantitative study can support national commissioning approval of PET-PSMA imaging agents. This outcome would reduce waiting lists and enhance clinical workflows for prostate cancer diagnosis and treatment.

Materials and Methods

A total of 61 [^{68}Ga]Ga-PSMA-11 and 72 ^{18}F-PSMA-1007 standard-of-care patients were scanned at our centre according to routine referral criteria for clinical indications

of suspected prostate cancer. The inclusion criteria comprised all consecutively scanned subjects identified in the PET imaging database. Patients with observed liver lesions were excluded from further analysis.

Subjects were analysed as two separate imaging-agent cohorts, each consisting of 200 suspected lesions, including metastatic sites of disease. Within the [^{68}Ga]Ga-PSMA-11 cohort, the mean ± standard deviation (SD) for weight, body surface area ($_{bsa}$), lean body mass ($_{lbm}$), injected activity, and uptake time were 86.1±16.9 kg, 2±0.2 m^2, 63.2±6.8 kg, 187.8±23.9 MBq, and 63.3±9.7 min, respectively. The same values in ^{18}F-PSMA-1007 subjects were 83.6±13.6 kg, 2±0.2 m2, 61.4±7.1 kg, 342±42 MBq, and 94.1±8 MBq, respectively.

Images were acquired using a BIOGRAPH mCT-S64 4R PET/CT scanner operating in step-and-shoot mode. Corrections for geometry, randoms, dead time, scatter, and attenuation were applied to the emission data. PET images were reconstructed using ordered-subsets expectation maximization with point-spread-function modeling and time-of-flight, using 2 iterations, 21 subsets, a 200 × 200 matrix, and a 5-mm FWHM Gaussian filter. Non-contrast CT scan parameters were as follows: 120 kVp; 10 mA for the topogram; 120 kVp with modulated mA; pitch of 0.8; and 3-mm CT slices. The scanner adhered to strict QC protocols, received manufacturer-recommended servicing, and was accredited annually under the Guy's and St Thomas' PET Core Lab national clinical trial programme.

Finalized clinical reports, created by PET/CT consultant radiologists, were reviewed by experienced PET physicists to identify the location of reported or suspected lesions. Lesion SUV_{max}, SUV_{mean}, standardized uptake value-peak (SUV_{peak}), SUV_{lbm}, and SUV_{bsa} normalizations were recorded for each imaging agent. Liver background SUV_{mean} was also noted, and the ratio of suspected lesion SUV_{max} to liver background SUV_{mean} was calculated to derive T/B ratios. Furthermore, functional volume-based surrogates metabolic tumor volume (MTV) and total lesion PSMA /(TL-PSMA) (i.e., MTV x lesion SUV_{mean}) were compared between the ^{18}F-PSMA-1007 and [^{68}Ga]Ga-PSMA-11 cohorts.

Siemens Syngo.viaTM imaging analysis software, with manual operator control, was used to record SUVs using different normalizations and to estimate MTV and TL-PSMA for each patient. The Shapiro-Wilk normality test in the StatsDirect™ statistical software package indicated that Mann-Whitney analysis should be used to identify significant differences between the distributions of [^{68}Ga]Ga-PSMA-11 and ^{18}F-PSMA-1007. A 95% confidence interval was used, and statistical significance was defined as $p<0.05$. This study was conducted as an anonymized clinical audit without the need for patient consent.

Results

A total of 133 patients and 400 suspected lesions, identified on ^{18}F-PSMA-1007 and [^{68}Ga]Ga-PSMA-11 PET/CT scans, were analysed. Results are presented in box-and-whisker plots (minimum, first quartile, median, third quartile, maximum), with the mean value denoted by X.

Suspected Lesion SUV

Statistically significant differences were observed in the distributions of SUV_{max} (p=0.0004), SUV_{peak} (p=0.0017), and SUV_{mean} (p=0.0007) between [^{68}Ga]Ga-PSMA-11 and ^{18}F-PSMA-1007 (Figure 1). These differences were also observed in SUV_{lbm} (p=0.0002) and SUV_{bsa} (p=0.0005) normalizations. In all cases, [^{68}Ga]Ga-PSMA-11 exhibited higher mean and median values than ^{18}F-PSMA-1007 (Figure 2).

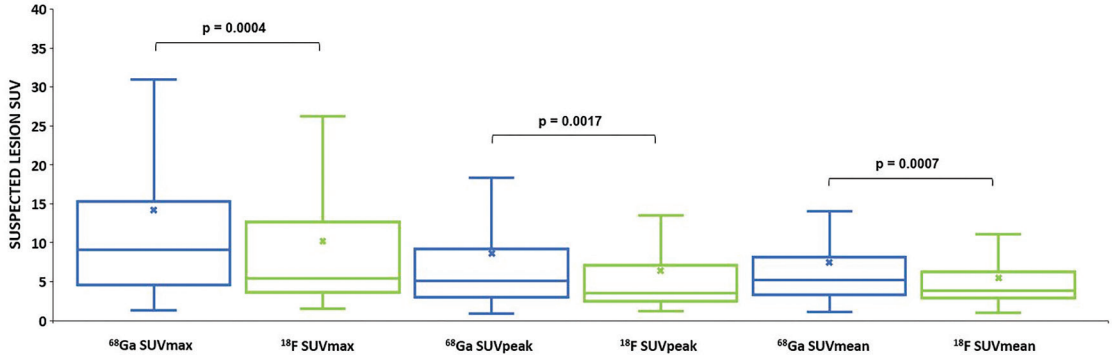

Figure 1. Suspected lesion SUV_{max}, SUV_{peak}, SUV_{mean} distributions in [^{68}Ga]Ga-PSMA-11 and ^{18}F-PSMA-1007 PET scans

SUV_{max}: Maximum standard uptake values, SUV_{mean}: Mean standardized uptake, SUV_{peak}: Standardized uptake value-peak, ^{18}F-PSMA: ^{18}F-prostate specific membrane antigen, PET: Positron emission tomography, SUV_{bsa}: Body surface area, SUV_{lsa}: Lean body mass

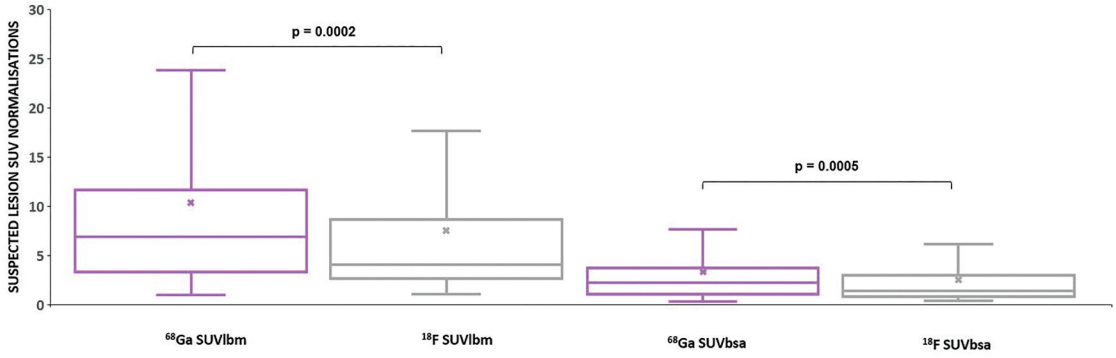

Figure 2. Suspected lesion SUV_{max} with lean body mass and surface area normalisation distributions in [^{68}Ga]Ga-PSMA-11 and ^{18}F-PSMA-1007 PET scans

SUV_{max}: Maximum standard uptake values, ^{18}F-PSMA: ^{18}F-prostate specific membrane antigen, PET: Positron emission tomography

Liver SUV

Liver SUV results showed highly significant differences between the distributions of [^{68}Ga]Ga-PSMA-11 and ^{18}F-PSMA-1007. Specifically, SUV_{max} ($p<0.0001$), SUV_{peak} ($p<0.0001$), and SUV_{mean} ($p<0.0001$) were higher for ^{18}F-PSMA-1007 than for [^{68}Ga]Ga-PSMA-11 (Figure 3).

T/B

T/B ratio distributions differed significantly ($p<0.0001$), with [^{68}Ga]Ga-PSMA-11 exhibiting higher mean and median values than ^{18}F-PSMA-1007 (Figure 4, left two datasets).

MTV

There was no significant difference in MTV distributions between [^{68}Ga]Ga-PSMA-11 and ^{18}F-PSMA-1007 ($p>0.05$; Figure 4, middle two datasets).

TL-PSMA

Significant differences were found in TL-PSMA distributions ($p=0.0063$), with [^{68}Ga]Ga-PSMA-11 exhibiting higher median and lower mean values compared to ^{18}F-PSMA-1007 Figure 4 (right 2 datasets).

%COV

Results indicated greater variability in [^{68}Ga]Ga-PSMA-11 distributions than in ^{18}F-PSMA-1007 for suspected lesion SUV (irrespective of normalisation), liver SUV_{mean}, and T/B. However, %COV for ^{18}FPSMA-1007 was higher for remaining liver SUV, MTV, and TL-PSMA volume estimations (Figure 5).

Discussion

Our centre initially used the widely available [^{68}Ga]Ga-PSMA-11 for prostate cancer imaging on PET/CT. However, logistical supply challenges, combined with substantially increased demand for scans led to long national delays in service delivery. As a result, together with others, we introduced ^{18}F-PSMA-1007 to address the backlog, and we now primarily use this imaging agent. The difference

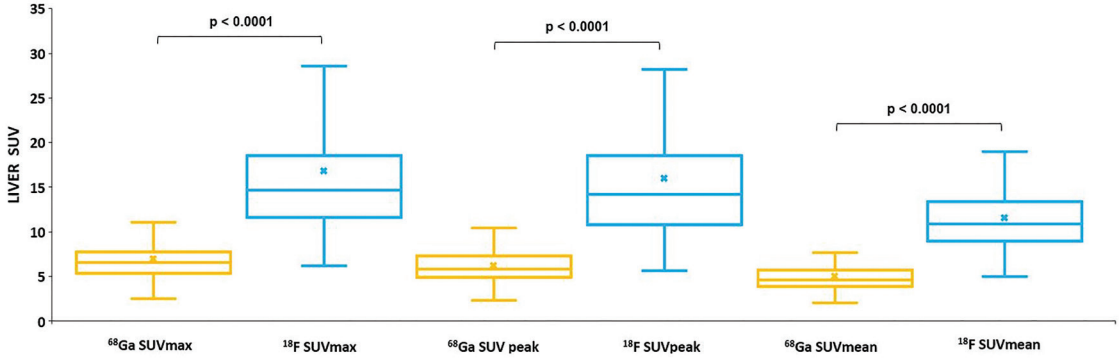

Figure 3. Background liver SUV_{mean} distributions in [^{68}Ga]Ga-PSMA-11 and ^{18}F-PSMA-1007 PET scans

SUV_{mean}: Mean standardized uptake, PSMA: Prostate specific membrane antigen, PET: Positron emission tomography, SUVmax: Maximum standard uptake values, SUVpeak: Standardized uptake value-peak

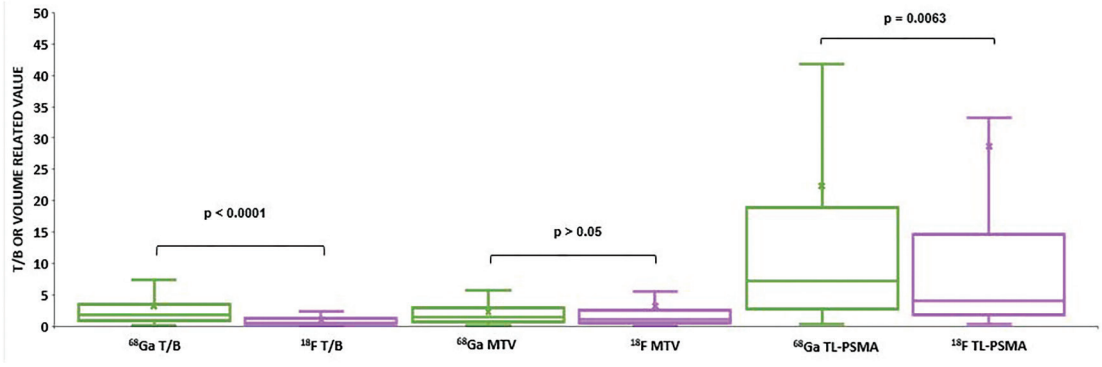

Figure 4. T/B, MTV and TL-PSMA distributions in [68Ga]Ga-PSMA-11 and 18F-PSMA-1007 PET scans

TL-PSMA: Total lesion prostate specific membrane antigen, PET: Positron emission tomography, T/B: Tumor-to-background, MTV: Metabolic tumor volume

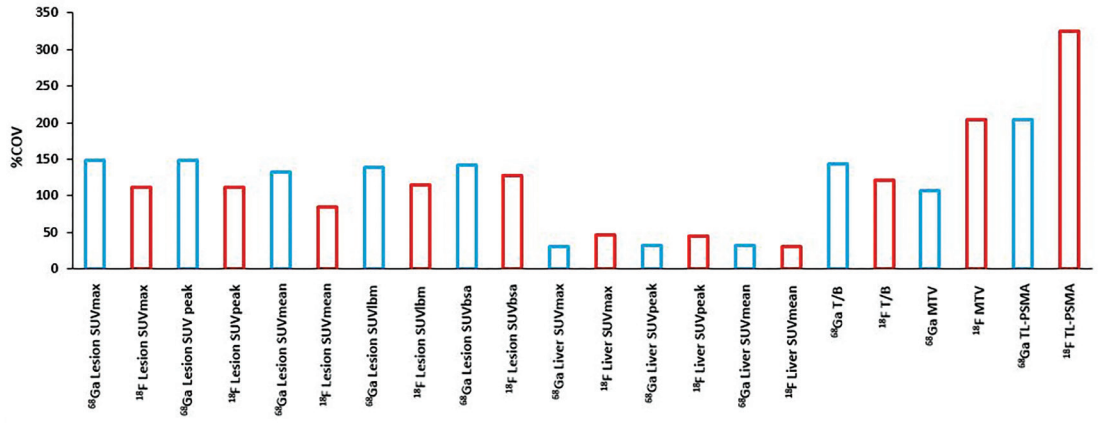

Figure 5. %COV of different parameters in [68Ga]Ga-PSMA-11 and 18F-PSMA-1007 PET scans

PSMA: Prostate specific membrane antigen, PET: Positron emission tomography

in cohort sizes in our study reflected the limited number of 68Ga PSMA patients scanned before the introduction of our 18F-PSMA service. The identical but larger number of lesions selected between tracers was intended to ensure good statistics by maximising the use of the available scan data. Lesions were selected directly from reports. It is recognised that injected activity regimes and uptake times differed between tracers, but each was optimised for service delivery and, accordingly, their differences were significant. Nevertheless, these logistical issues do not impact the efficacy of this study, as the same protocols were used throughout for each tracer and the study was performed on a single machine. Indeed, many centres routinely exchange these imaging agents to optimise service delivery when tracer supply is compromised, taking these considerations into account.

Despite the potential for interchangeability of [68Ga]Ga-PSMA-11 and 18F-PSMA-1007 imaging agents in clinical practice (17), relatively few studies have conducted direct, matched comparisons (18,19). Furthermore, publications often compare different clinical metrics of efficacy (20), including qualitative interpretations. We characterise PSMA uptake of [68Ga]Ga-PSMA-11 and 18F-PSMA-1007, focusing on quantitative SUV, T/B, and volume-surrogate differences when these tracers are interchanged due to supply issues.

Suspected lesion SUV

In this study, significant differences were observed between the two tracers in SUV_{max}, SUV_{peak}, SUV_{mean}, SUV_{lbm}, and SUV_{bsa}, with [68Ga]Ga-PSMA-11 showing higher values (Figures 1, 2). However, in a different consecutive-scan PSMA study using 18F-PSMA-1007 and [68Ga]Ga-PSMA-11 (21) with 46 patients, no significant differences were seen in median SUV_{max} or SUV_{peak} for suspected prostate, lymph nodes, or metastatic bone disease. Similarly, no significant differences were observed in the median SUV_{max} between radiopharmaceuticals in another biopsy-proven study of

40 patients (22). Alternatively, in a separate study (17) of 16 patients, the median SUV_{max} of primary prostate lesions was greater for ^{18}F-PSMA-1007 than for [^{68}Ga]Ga-PSMA-11 (p=0.002).

Differences in results between studies may highlight variability in study design, patient recruitment, disease stage, acquisition protocols, reversibility of kinetics in organs/lesions (23), and various analysis techniques. Therefore, these issues should be considered when comparing studies and drawing conclusions.

Liver SUV

Our results showed that the ^{18}F-PSMA-1007 SUV_{mean} of normal liver background tissue was significantly higher than the corresponding value for [^{68}Ga]Ga-PSMA-11 (Figure 3), and this outcome agreed with other studies (24). As such, interchanging imaging agents would affect T/B ratios when the liver is chosen as the background. Conversely, differences are predictable, and it may be possible to derive a correction factor between interchanged radiopharmaceuticals if patient selection T/B criteria are met.

T/B

Our results (Figure 4) showed that [^{68}Ga]Ga-PSMA-11 exhibited significantly higher mean and median lesion-to-liver ratio values compared with [^{18}F]PSMA-1007, resulting in a [^{68}Ga]Ga-PSMA-11 mean T/B approximately 3 times that of ^{18}F-PSMA-1007.

However, others have noted that when the spleen (21,24,25) is used for background, ^{18}F-PSMA-1007 uptake is much higher than liver ^{68}Ga uptake, and the range is greater for ^{18}F-PSMA-1007 and [^{68}Ga]Ga-PSMA-11 compared with hepatic PSMA uptake. Another study (17) reported that background median SUV_{max} was greater for ^{18}F-PSMA-1007 than for [^{68}Ga]Ga-PSMA-11 in the gluteus maximus (p=0.001) and in the blood pool (p=0.001). They showed no significant differences in any T/B ratios between imaging agents. Similarly, consideration of these issues is recommended when comparing studies and drawing conclusions, especially regarding patient selection criteria in trials.

This challenge also applies to the VISION prostate cancer trial, in which patients with metastatic castration-resistant prostate cancer received ^{177}Lu-PSMA-617 therapy. One eligibility criterion was a PSMA-positive [^{68}Ga]Ga-PSMA-11 PET/CT scan, defined by a lesion-to-liver uptake ratio >1. In our study, this suggested 150 of the 200 [^{68}Ga]Ga-PSMA-11patients (i.e. 75%) would be eligible ideally if all other criteria were met. Hypothetically, if the VISION study [^{68}Ga]Ga-PSMA-11 patient-selection criterion (T/B >1) were applied to our ^{18}F-PSMA-1007 T/B data, this would imply that 62 of the 200 ^{18}F-PSMA-1007 therapy patients (31%) would be eligible. This represents a 59% difference between the tracers at the same [^{68}Ga]Ga-PSMA-11 T/B ratio threshold. However, it is acknowledged that different biodistributions predominate, and that the refined VISION trial therapy eligibility conditions differed from the broader standard-of-care requirements under which scans were acquired here. These differences highlight the need for careful consideration and caution when tracers are interchanged, for example, due to supply issues.

Furthermore, in our study, we observed significant differences in lesion SUV, liver SUV, T/B, and TL-PSMA between tracers, with mean ± SD values presented in Table 1. However, one must exercise caution when making direct comparisons between tracers using such metrics because bias may influence the results. Knowledge of all influencing factors is essential for a fully valid assessment of clinical efficacy, including tumour stage, recurrence, PSA, injected activity, acquisition protocols, image reconstruction techniques, sample size, and treatments, among others. Reviews in this area (26) have shown that [^{68}Ga]Ga-PSMA-11 exhibits high urinary tract excretion and may complicate the diagnosis of small lesions near the prostate bed or bladder. While ^{18}F-PSMA-1007 is dominated by hepatobiliary excretion with potential for improved ability to identify lesions in the pelvic region. Moreover, others have shown that the sensitivity of [^{68}Ga]Ga-PSMA-11 may be slightly lower than that of [^{18}F]PSMA-1007 for detecting small lesions or at very low PSA levels. [^{68}Ga]Ga-PSMA-11 may benefit from a lower false-positive rate in bone and ganglia compared with [^{18}F]PSMA-1007.

Table 1. Mean with standard deviation of some parameters investigated which demonstrated significant difference

	Mean ± SD	Tracer
Lesion	14.23±21.14	[^{68}Ga]Ga-PSMA-11
SUV_{max}	10.2±11.37	^{18}F-PSMA-1007
Lesion	7.44±9.87	[^{68}Ga]Ga-PSMA-11
SUV_{mean}	5.51±4.68	^{18}F-PSMA-1007
Liver	5.02±1.59	[^{68}Ga]Ga-PSMA-11
SUV_{mean}	11.57±3.53	^{18}F-PSMA-1007
T/B	3.24±4.65	[^{68}Ga]Ga-PSMA-11
	1.01±1.22	^{18}F-PSMA-1007
TLG	22.31±45.7	[^{68}Ga]Ga-PSMA-11
	28.75±93.26	^{18}F-PSMA-1007

SUV_{max}: Maximum standard uptake values, SUV_{mean}: Maximum standard uptake values, T/B: Tumor-to-background, TLG: Total lesion glycolysis, SD: Standard deviation, PSMA: Prostate specific membrane antigen

Although differences in results are seen in many published studies, and some are contradictory, the consensus is that both tracers exhibit comparable diagnostic performance in the clinical setting. Local validation of equivalence in tracer exchange is highly recommended to ensure that any departure from expectations is understood. Caution is also advised in clinical trials, particularly if patient recruitment is based on retrospective standard-of-care scans involving, for example, the lesion T/B ratio.

MTV and TL-PSMA

In this study, no significant difference was recorded in MTV between tracers. Estimation of MTV arises from a convolution of factors, including the software algorithm used to derive it, lesion SUV_{max}, lesion homogeneity or heterogeneity, and neighbouring tissue uptake. With this understanding, the MTV was not statistically significant in our case.

The TL-PSMA is estimated as the product of MTV and lesion SUV_{mean}. In our case, the lesion SUV_{mean} was significantly different between tracers. A Higher lesion SUV_{mean} associated with [68Ga]Ga-PSMA-11, compared with 18F-PSMA-1007, likely contributed to this result. Supporting this, another 42-patient study found that a significant difference in TL-PSMA between tracers enabled the prediction of a high Gleason score in favour of 18F-PSMA-1007 (27).

%COV

We presented diverse %COV results across the quantitative parameters investigated, implying the absence of overall superiority of either PSMA imaging agent. In all cases, the %COV for background liver revealed that 18F-PSMA-1007 was higher than [68Ga]Ga-PSMA-11, while for suspected lesions [68Ga]Ga-PSMA-11 was higher than 18F-PSMA-1007; across parameters studied, the %COV for suspected lesions was higher than that for liver. These findings also confirm results reported by others (24).

In summary, for our entire study, we characterised 18F-PSMA-1007 and [68Ga]Ga-PSMA-11 PET PSMA-suspected lesion SUV, background liver SUV, T/B ratios, and %COV at our centre, and demonstrated that quantitative PET measurements are of the same order of magnitude, while quantitative differences are generally consistent and predictable. Our results, obtained using these imaging agents, support their interchangeability during supply shortages and are consistent with other studies, e.g. (4). We also provide further support for the existing evidence base that supports the national regulatory approval of PET PSMA imaging agents, such as 18F-PSMA-1007, in France in 2021 (28). Indeed, NHS England in 2025 recognised this necessity with commissioning policy approval for PSMA PET e.g. [68Ga]Ga-PSMA-11 and 18F-PSMA-1007 in prostate cancer to ameliorate tracer availability challenges (29).

However, important caveats must be considered when exchanging tracers, particularly in applications such as PSMA radioligand therapy (30,31), including more recent [161Tb]Tb-PSMA (32) and [225Ac]Ac-PSMA (33), where patient therapy selection using T/B ratios may be influenced by individual variations in radiopharmaceutical biodistribution, tissue uptake, and, particularly, background selection.

Study Limitations

This was a single-centre retrospective audit in which all suspicious lesions were identified by reporting radiologists as part of standard-of-care practice. We included all suspected prostate cancer referrals and analysed clinically reported suspected lesions to provide a more realistic system-level quantitative characterization, rather than identifying specific tumour types or sites for analysis, because of the possibility of reduced statistical power. Similarly, PSA levels were not included in reports, and were therefore unavailable for this audit. However, the interchange of tracers is vital for many centres to maintain delivery of prostate cancer imaging services throughout the patient pathway, irrespective of PSA levels, because national demand for diagnosis remains very high. Other constraints in this study include the lack of histological confirmation; therefore, we refer to suspected lesions. Patient cohorts received one radiopharmaceutical but not the other, limiting the ability to make a fully matched comparison. Although hepatic lesions were excluded from the analysis, residual bias may remain in cases where clinicians could not visually identify such lesions. However, scans were interpreted by trained radiologists, and experienced PET physicists conducted data analysis to ensure the validity of the findings.

Overall, we believe that we have satisfied the quantitative case for interchange between [68Ga]Ga-PSMA-11 and 18F-PSMA-1007 tracers for routine use in referrals for suspected prostate cancer, and we support national recommendations that advocate PET PSMA.

Conclusion

We characterised significant differences in [68Ga]Ga-PSMA-11 and 18F-PSMA-1007 PET PSMA suspected prostate cancer patients for suspected lesion SUV_{max} ($p=0.0004$), SUV_{peak} ($p=0.0017$), SUV_{mean} ($p=0.0007$), SUV_{lbm} ($p=0.0002$) and SUV_{bsa} ($p=0.0005$) with higher [68Ga]Ga-PSMA-11 values. Similarly, for background liver, we confirmed higher SUV_{max} ($p<0.0001$), SUV_{peak} ($p<0.0001$), and SUV_{mean}

(p<0.0001) with ^{18}F-PSMA-1007. We also identified significant differences in T/B (p<0.0001) and in TL-PSMA (p=0.0063). Our results favour adopting these PSMA tracers for routine clinical use in PET for prostate cancer and further support the new NHS England commissioning policy.

Ethics

Ethics Committee Approval: This study was conducted as an anonymised audit and as such ethics was not required.

Informed Consent: This study was conducted as an anonymised audit and as such informed consent was not required.

Footnotes

Authorship Contributions

Concept: B.S., G.L., S.S., W.L.W., Design: B.S., G.L., S.S., W.L.W., Data Collection or Processing: B.S., G.L., S.S., W.L.W., Analysis or Interpretation: B.S., G.L., S.S., W.L.W., Literature Search: B.S., G.L., S.S., W.L.W., Writing: B.S., G.L., S.S., W.L.W.z

Conflict of Interest: No conflict of interest was declared by the authors.

Financial Disclosure: The authors declared that this study has received no financial support.

References

1. Tan EH, Burn E, Barclay NL, Delmestri A, Man WY, Golozar A, Serrano ÀR, Duarte-Salles T, Cornford P, Prieto Alhambra D, Newby D; OPTIMA Consortium. Incidence, prevalence, and survival of prostate cancer in the UK. JAMA Netw Open. 2024;7:e2434622.
2. Shen K, Liu B, Zhou X, Ji Y, Chen L, Wang Q, Xue W. The evolving role of ^{18}F-FDG PET/CT in diagnosis and prognosis prediction in progressive prostate cancer. Front Oncol. 2021;11:683793.
3. Ilhan H, Royce T, Qiu X, Zamboglou C. Editorial: exploring the potential of PSMA-PET imaging on personalized prostate cancer treatment. Front Oncol. 2022;12:832747.
4. Huang S, Ong S, McKenzie D, Mirabelli A, Chen DC, Chengodu T, Murphy DG, Hofman MS, Lawrentschuk N, Perera M. Comparison of ^{18}F-based PSMA radiotracers with [^{68}Ga]Ga-PSMA-11 in PET/CT imaging of prostate cancer-a systematic review and meta-analysis. Prostate Cancer Prostatic Dis. 2024;27:654-664.
5. Giunta EF, Brighi N, Gurioli G, Matteucci F, Paganelli G, De Giorgi U. ^{177}Lu-PSMA therapy in metastatic prostate cancer: an updated review of prognostic and predictive biomarkers. Cancer Treat Rev. 2024;125:102699.
6. Rowe SP, Buck A, Bundschuh RA, Lapa C, Serfling SE, Derlin T, Higuchi T, Gorin MA, Pomper MG, Werner RA. [^{18}F]DCFPyL PET/CT for imaging of prostate cancer. Nuklearmedizin. 2022;61:240-246.
7. Vázquez SM, Endepols H, Fischer T, Tawadros SG, Hohberg M, Zimmermanns B, Dietlein F, Neumaier B, Drzezga A, Dietlein M, Schomäcker K. Translational development of a Zr-89-labeled inhibitor of prostate-specific membrane antigen for PET imaging in prostate cancer. Mol Imaging Biol. 2022;24:115-125.
8. Naik M, Khan SR, Lewington V, Challapalli A, Eccles A, Barwick TD. Imaging and therapy in prostate cancer using prostate specific membrane antigen radioligands. Br J Radiol. 2024;97:1391-1404.
9. Rosar F, Burgard C, David S, Marlowe RJ, Bartholomä M, Maus S, Petto S, Khreish F, Schaefer-Schuler A, Ezziddin S. Dual FDG/PSMA PET imaging to predict lesion-based progression of mCRPC during PSMA-RLT. Sci Rep. 2024;14:11271.
10. Wang Q, Ketteler S, Bagheri S, Ebrahimifard A, Luster M, Librizzi D, Yousefi BH. Diagnostic efficacy of [^{99m}Tc]Tc-PSMA SPECT/CT for prostate cancer: a meta-analysis. BMC Cancer. 2024;24:982.
11. Aksu A, Çapa Kaya G. Is SUV Corrected for lean body mass superior to SUV of body weight in ^{68}Ga-PSMA PET/CT? Mol Imaging Radionucl Ther. 2021;30:144-149.
12. Bela Andela S, Amthauer H, Furth C, Rogasch JM, Beck M, Mehrhof F, Ghadjar P, van den Hoff J, Klatte T, Tahbaz R, Zips D, Hofheinz F, Zschaeck S. Quantitative PSMA-PET parameters in localized prostate cancer: prognostic and potential predictive value. Radiat Oncol. 2024;19:97.
13. Sartor O, de Bono J, Chi KN, Fizazi K, Herrmann K, Rahbar K, Tagawa ST, Nordquist LT, Vaishampayan N, El-Haddad G, Park CH, Beer TM, Armour A, Pérez-Contreras WJ, DeSilvio M, Kpamegan E, Gericke G, Messmann RA, Morris MJ, Krause BJ; VISION investigators. lutetium-177-PSMA-617 for metastatic castration-resistant prostate cancer. N Engl J Med. 2021;385:1091-1103.
14. Kuo PH, Benson T, Messmann R, Groaning M. Why we did what we did: PSMA PET/CT selection criteria for the VISION Trial. J Nucl Med. 2022;63:816-818.
15. Cook GJR, Wong WL, Sanghera B, Mangar S, Challapalli A, Bahl A, Bassett P, Leaning D, Schmidkonz C. Eligibility for ^{177}Lu-PSMA therapy depends on the choice of companion diagnostic tracer: a comparison of ^{68}Ga-PSMA-11 and ^{99m}Tc-MIP-1404 in metastatic castration-resistant prostate cancer. J Nucl Med. 2023;64:227-231.
16. Ahmadzadehfar H, Seifert R, Afshar-Oromieh A, Kratochwil C, Rahbar K. Prostate cancer theranostics with ^{177}Lu-PSMA. Semin Nucl Med. 2024;54:581-590.
17. Kuten J, Fahoum I, Savin Z, Shamni O, Gitstein G, Hershkovitz D, Mabjeesh NJ, Yossepowitch O, Mishani E, Even-Sapir E. Head-to-head comparison of ^{68}Ga-PSMA-11 with ^{18}F-PSMA-1007 PET/CT in staging prostate cancer using histopathology and immunohistochemical analysis as a reference standard. J Nucl Med. 2020;61:527-532.
18. Evangelista L, Maurer T, van der Poel H, Alongi F, Kunikowska J, Laudicella R, Fanti S, Hofman MS. [^{68}Ga]Ga-PSMA versus [^{18}F]PSMA positron emission tomography/computed tomography in the staging of primary and recurrent prostate cancer. A systematic review of the literature. Eur Urol Oncol. 2022;5:273-282.
19. De Man K, Van Laeken N, Schelfhout V, Fendler WP, Lambert B, Kersemans K, Piron S, Lumen N, Decaestecker K, Fonteyne V, Delrue L, De Vos F, Ost P. ^{18}F-PSMA-11 versus ^{68}Ga-PSMA-11 positron emission tomography/computed tomography for staging and biochemical recurrence of prostate cancer: a prospective double-blind randomised cross-over trial. Eur Urol. 2022;82:501-509.
20. Hoffmann MA, Müller-Hübenthal J, Rosar F, Fischer N, von Eyben FE, Buchholz HG, Wieler HJ, Schreckenberger M. Primary staging of prostate cancer patients with [^{18}F]PSMA-1007 PET/CT compared with [^{68}Ga]Ga-PSMA-11 PET/CT. J Clin Med. 2022;11:5064.
21. Hoberück S, Löck S, Borkowetz A, Sommer U, Winzer R, Zöphel K, Fedders D, Michler E, Kotzerke J, Kopka K, Hölscher T, Braune A. Intraindividual comparison of [^{68} Ga]-Ga-PSMA-11 and [^{18}F]-F-PSMA-1007 in prostate cancer patients: a retrospective single-center analysis. EJNMMI Res. 2021;11:109.
22. Chandekar KR, Singh H, Kumar R, Kumar S, Kakkar N, Mittal BR, Singh SK. Comparison of 18 F-PSMA-1007 PET/CT with 68 Ga-PSMA-11 PET/CT for initial staging in intermediate- and high-risk prostate cancer. Clin Nucl Med. 2023;48:e1-e8.
23. Dias AH, Jochumsen MR, Zacho HD, Munk OL, Gormsen LC. Multiparametric dynamic whole-body PSMA PET/CT using [^{68}Ga]Ga-PSMA-11 and [^{18}F]PSMA-1007. EJNMMI Res. 2023;13:31.

24. Popescu CE, Zhang B, Sartoretti T, Spielhofer N, Skawran S, Heimer J, Messerli M, Sauter A, Huellner MW, Kaufmann PA, Burger IA, Maurer A. Evaluating the biodistribution for [68Ga]Ga-PSMA-11 and [18F]F-PSMA-1007 PET/CT with an inter- and intrapatient based analysis. EJNMMI Res. 2024;14:36.
25. Seifert R, Telli T, Hadaschik B, Fendler WP, Kuo PH, Herrmann K. Is 18F-FDG PET needed to assess 177Lu-PSMA therapy eligibility? A VISION-like, single-center analysis. J Nucl Med. 2023;64:731-737.
26. Abdi N, Alsulami M, Ghaznavi H. Comparing the diagnostic performance of [18F]PSMA-1007 with [68Ga]Ga-PSMA-11 in PET/CT imaging and staging of recurrent prostate cancer. Med Adv. 2025;3:9-19.
27. Pizzuto DA, Guerreri M, Zamboglou C, Boldrini L, Gatta R, Ruggierro M, De Summa M, Caldarella C, Annunziata S. The clinical predictive value of radiomic features from [68Ga]Ga-PSMA-11 and [18F]F-PSMA-1007 PET in patients with prostate cancer: a preliminary comparative study. Clin Transl Imaging 2024;12:629-638.
28. (ANSM) Andsdmedpds. Protocole D'utilisation therapeutique et de Recueil D'informations ABX-PSMA-1007, 1300 MBq/mL solution injectable, substance active: [18F]PSMA-1007. 2010. Available from: http://agence-prd.ansm.sante.fr/php/ecodex/extrait.php?specid=64034289.
29. Public Health Evidence Report 2307. Prostate-specific membrane antigen (PSMA) radiotracers in positron emission tomography – computed tomography (PETCT) imaging for individuals with high-risk primary or recurrent prostate cancer (adults). (2025, February). NHS England.
30. Kind F, Eder AC, Jilg CA, Hartrampf PE, Meyer PT, Ruf J, Michalski K. Prognostic value of tumor volume assessment on PSMA PET After 177Lu-PSMA radioligand therapy evaluated by PSMA PET/ct consensus statement and RECIP 1.0. J Nucl Med. 2023;64:605-610.
31. Fendler WP, Eiber M, Beheshti M, Bomanji J, Calais J, Ceci F, Cho SY, Fanti S, Giesel FL, Goffin K, Haberkorn U, Jacene H, Koo PJ, Kopka K, Krause BJ, Lindenberg L, Marcus C, Mottaghy FM, Oprea-Lager DE, Osborne JR, Piert M, Rowe SP, Schöder H, Wan S, Wester HJ, Hope TA, Herrmann K. PSMA PET/CT: joint EANM procedure guideline/SNMMI procedure standard for prostate cancer imaging 2.0. Eur J Nucl Med Mol Imaging. 2023;50:1466-1486.
32. Abdlkadir AS, Rosar F, Jalilian A, Moghrabi S, Al-Balooshi B, Rabei O, Kairemo K, Al-Ibraheem A. Harnessing terbium radioisotopes for clinical advancements: a systematic review. Nucl Med Mol Imaging. 2025;59:50-61.
33. Sathekge MM, Lawal IO, Bal C, Bruchertseifer F, Ballal S, Cardaci G, Davis C, Eiber M, Hekimsoy T, Knoesen O, Kratochwil C, Lenzo NP, Mahapane J, Maserumule LC, Mdlophane AH, Mokoala KMG, Ndlovu H, Pant V, Rathke H, Reed J, Sen IB, Singh A, Sood A, Tauber R, Thakral P, Yadav MP, Morgenstern A. Actinium-225-PSMA radioligand therapy of metastatic castration-resistant prostate cancer (WARMTH Act): a multicentre, retrospective study. Lancet Oncol. 2024;25:175-183.